Effective Preconditioners for the Solution of Hybrid FEM/MoM Matrix Equations using Combined Formulations

Chunlei Guo and Todd H. Hubing
Department of Electrical and Computer Engineering
University of Missouri-Rolla
Rolla, MO 65409

ABSTRACT

Hybrid FEM/MoM modeling codes generate large systems of equations that are generally solved using inward-looking, outward-looking or combined formulations. For many types of problems, the combined formulation is preferred because it does not require a direct inversion of the coefficient matrices and can be solved using iterative solution techniques. An effective preconditioner is a crucial part of the solution process in order to guarantee convergence. However, it can be difficult to generate effective, memory-efficient preconditioners for large problems. This paper investigates preconditioners that use the FEM solution and an absorbing boundary condition (ABC). Various techniques are explored to reduce the memory required by the preconditioner while maintaining effectiveness. Practical problems are presented to evaluate the effectiveness of these preconditioners in various situations.

I. INTRODUCTION

The hybrid finite-element-method/method-of-moments (FEM/MoM) combines the finite element method (FEM) and the method of moments (MoM) and has been used to analyze signal integrity (SI) [1], electromagnetic scattering, and radiation problems [2–6]. FEM is used to model structures with geometrical complexity and inhomogeneous materials. MoM is used to model larger metallic structures and to provide an exact radiation boundary condition (RBC) to terminate the FEM mesh. These two methods are coupled by enforcing field continuity on the boundary separating the FEM and MoM regions.

There are three ways of formulating hybrid FEM/MoM methods [7–9]. The outward-looking formulation constructs an RBC from MoM and incorporates it into the FEM equations. This formulation has been used by Ji *et al*. [9], Jin and Volakis [10], and Ramahi and Mittra [11]. The inward-looking formulation incorporates an RBC constructed from FEM into the MoM equations. This formulation has been utilized by Jin and Liepa [12], Yuan *et al*. [13], and Sheng *et al*. [14]. These two formulations usually involve direct or indirect inversion of the FEM or MoM matrices, so they can be computationally expensive. The combined formulation, on the other hand, combines the FEM and MoM equations and solves for all unknowns at the same time using an iterative solver without requiring a direct matrix inversion. This formulation has been employed by Sheng *et al*. [18]. Techniques to reduce the complexity of the matrix-vector multiplication associated with the MoM part, such as the fast multipole method (FMM) [15, 28], multilevel fast multipole algorithm (MLFMA) [16], and adaptive integral method (AIM) [17], can be readily incorporated into a combined formulation.

The matrix equation generated using the combined formulation is partly full and partly sparse. This matrix is usually ill-conditioned, and the iterative solver may converge very slowly or not at all without an effective preconditioner. An effective preconditioner can reduce the necessary iterations dramatically, resulting in a significant reduction in the overall simulation time. Thus, a preconditioner is a crucial part of the iterative solution. Generally a more accurate approximation of the system results in a more effective preconditioner.

A major feature of a preconditioner is its memory efficiency. In most cases, a preconditioner which utilizes less memory can be developed using a less accurate approximation of the original system. However, this may cause the iterative solver to require more steps to converge; so there is usually a tradeoff between the speed and the memory-efficiency of a preconditioner.

For a system with a small number of unknowns (e.g. 10^3), it is relatively easy to use the complete or incomplete LU (ILU) decomposition of the hybrid

matrix to make an effective preconditioner without exceeding the memory available on typical personal computers. For a system with a large number of unknowns (e.g. 10^6), FMM or similar techniques can be used to reduce the memory requirement. Diagonal, block-diagonal, or near-neighbor matrices are often used to build preconditioners [17], but such preconditioners do not usually yield the most efficient solution. In [19], Liu and Jin proposed a preconditioner using a sparse matrix generated by FEM and an absorbing boundary condition (ABC). This preconditioner was shown to improve the convergence of iterative solvers greatly. This paper further investigates the FEM/ABC preconditioner and proposes a modified preconditioner for geometries with large metallic surfaces.

Section II of this paper presents the necessary formulations. Representative examples are introduced in Section III. Reordering techniques to reduce the number of fill-in elements in ILU decompositions are discussed in Section IV and a modified preconditioner that further reduces the memory requirement is proposed. Finally, conclusions from the work presented here are drawn in Section V.

II. FORMULATIONS

The Hybrid FEM/MoM Using the Combined Formulation

In the hybrid FEM/MoM, an electromagnetic problem is divided into an interior equivalent part and an exterior equivalent part. The interior part is modeled using the FEM and the exterior part is modeled using a surface integral equation method. The two parts are coupled by enforcing the continuity of tangential fields on the FEM and MoM boundary. FEM can be used to analyze the interior equivalent part and generates a sparse matrix equation of the form,

$$\begin{bmatrix} A_{ii} & A_{is} \\ A_{si} & A_{ss} \end{bmatrix} \begin{bmatrix} E_i \\ E_s \end{bmatrix} = \begin{bmatrix} 0 & 0 \\ 0 & B_{ss} \end{bmatrix} \begin{bmatrix} 0 \\ J_s \end{bmatrix} + \begin{bmatrix} g_i \\ g_s \end{bmatrix}. \quad (1)$$

A detailed explanation of Equation (1) can be found in [9].

The exterior equivalent problem can be analyzed by using an electric field integral equation (EFIE), magnetic field integral equation (MFIE), or a combined field integral equation (CFIE), which is a linear combination of the EFIE and MFIE. Regardless of the choice of testing functions or integral equations, the MoM matrix equation has the following form [9],

$$\begin{bmatrix} C \end{bmatrix} \begin{bmatrix} J_s \end{bmatrix} = \begin{bmatrix} D \end{bmatrix} \begin{bmatrix} E_s \end{bmatrix} - \begin{bmatrix} F \end{bmatrix} \quad (2)$$

where J_s is a set of unknown complex scalar coefficients, C and D are dense coefficient matrices, and F is the combined source term specifically given by [20],

$$F_m = \int_{S_m} \mathbf{f}_m(\mathbf{r}) \bullet \left[\mathbf{E}^{inc}(\mathbf{r}) + \eta_0 \hat{n} \times \mathbf{H}^{inc}(\mathbf{r}) \right] dS \quad (3)$$

where $f_m(r)$ is the set of basis functions on the surface and $\hat{n}$ is a unit normal vector pointing outward from the surface S.

Neither Equation (1) nor Equation (2) can be solved independently. These two equations form a coupled and determined system. The combined formulation is obtained from Equations (1) and (2) as,

$$\begin{bmatrix} A_{ii} & A_{is} & 0 \\ A_{si} & A_{ss} & -B_{ss} \\ 0 & D & -C \end{bmatrix} \begin{bmatrix} E_i \\ E_s \\ J_s \end{bmatrix} = \begin{bmatrix} g_i \\ g_s \\ F \end{bmatrix}. \quad (4)$$

Unlike the inward-looking formulation or the outward-looking formulation, the combined formulation doesn't require an explicit inversion of any matrix and solves for all the unknowns simultaneously. For many configurations, with proper preconditioning, the combined formulation is the most computationally efficient of the three formulations.

Equation (4) can be written in the form,

$$Mx = b \quad (5)$$

where

$$M = \begin{bmatrix} A_{ii} & A_{is} & 0 \\ A_{si} & A_{ss} & -B_{ss} \\ 0 & D & -C \end{bmatrix} \quad (6)$$

$x = \begin{bmatrix} E_i & E_s & J_s \end{bmatrix}^T$, and $b = \begin{bmatrix} g_i & g_s & F \end{bmatrix}^T$. Notice that the matrix M is a hybrid matrix, which is partly full and partly sparse. The convergence rate of an iterative solver for Equation (5) is highly dependent on the condition number of M.

The matrix M usually has a very large condition number (e.g. on the order of 10^6 or higher), which results in poor convergence or non-convergence of the iterative solution. However, Equation (5) can be transformed into another linear equation with the same solution,

$$PMx = Pb \qquad (7)$$

where $P \approx M^{-1}$ is a preconditioner matrix. With the proper choice of P, the matrix PM has better spectral properties than M and the number of iterations required to converge is greatly reduced. Ideally, the construction and application of a good preconditioner should be fast without requiring a lot of memory.

Application of FEM and ABC as a Preconditioner

Liu and Jin proposed a preconditioner that applies an absorbing boundary condition on the truncation surface to approximate the MoM boundary condition [19]. A sparse preconditioning matrix can be formed by replacing the EFIE or MFIE equations with first-order ABCs [8] on the truncation surface S,

$$\hat{n} \times \nabla \times \boldsymbol{E}^s\left(\boldsymbol{r}\right) = jk_0 \boldsymbol{E}^s\left(\boldsymbol{r}\right), \ \boldsymbol{r} \in S \qquad (8)$$

where $\boldsymbol{E}^s = \boldsymbol{E} - \boldsymbol{E}^{inc}$ is the scattered electric field. From Equation (8) we can derive,

$$\boldsymbol{E}(\boldsymbol{r}) + \eta_0 \hat{n} \times \boldsymbol{H}(\boldsymbol{r}) =$$
$$\boldsymbol{E}^{inc}(\boldsymbol{r}) + \eta_0 \hat{n} \times \boldsymbol{H}^{inc}(\boldsymbol{r}), \quad \boldsymbol{r} \in S. \qquad (9)$$

The same basis functions on the surface S used in the hybrid FEM/MoM method can be applied to approximate the **E** and **H** fields in Equation (9), and the basis functions $\boldsymbol{f}_m(\boldsymbol{r})$ can be used to test Equation (9), resulting in a matrix equation of the form,

$$\left[B_{ss}^T \right]\left[E_s \right] + \left[H_{ss} \right]\left[J_s \right] = \left[L \right] \qquad (10)$$

where $\left[B_{ss}^T \right]$ is the transpose of the matrix B_{ss} in Equation (1), H_{ss} is given by

$$\left[H_{ss} \right]_{mn} = \int_{S_m} \eta_0 \boldsymbol{f}_m(\boldsymbol{r}) \bullet \boldsymbol{f}_n(\boldsymbol{r}) dS \qquad (11)$$

and L is the source term given by,

$$L_m = \int_{S_m} \boldsymbol{f}_m(\boldsymbol{r}) \bullet \boldsymbol{E}^{inc}(\boldsymbol{r}) dS$$
$$+ \eta_0 \int_{S_m} \boldsymbol{f}_m(\boldsymbol{r}) \bullet \hat{n} \times \boldsymbol{H}^{inc}(\boldsymbol{r}) dS. \qquad (12)$$

The ABC approximates the MoM boundary condition described using the TENH form of the CFIE.

Combining Equation (10) with Equation (1), we have,

$$\begin{bmatrix} A_{ii} & A_{is} & 0 \\ A_{si} & A_{ss} & -B_{ss} \\ 0 & B_{ss}^T & H_{ss} \end{bmatrix} \begin{bmatrix} E_i \\ E_s \\ J_s \end{bmatrix} = \begin{bmatrix} g_i \\ g_s \\ K \end{bmatrix} \qquad (13)$$

and we define

$$Q = \begin{bmatrix} A_{ii} & A_{is} & 0 \\ A_{si} & A_{ss} & -B_{ss} \\ 0 & B_{ss}^T & H_{ss} \end{bmatrix}. \qquad (14)$$

Notice that the matrix Q is very sparse. Now we have two systems: the hybrid FEM/MoM system described by Equation (4) and the FEM/ABC system described by Equation (13).

Since Equation (8) describes the behavior of the electric field in free space far from the sources, the ABC truncation surface should not be too close to the scatterer. When the ABC truncation surface is far enough from the scatterer's surface (e.g. $\lambda/10$), the FEM/ABC system described by Equation (13) can be a good physical approximation of the hybrid system described by Equation (4).

If the same computational domain is analyzed using both Equations (4) and (13), the matrix M is of the same order as the matrix Q. The matrix Q is a physical approximation of M, and Q^{-1} can be used as a preconditioner to improve the iterative solution of Equation (6). Q is highly sparse, and doesn't require much additional memory. Q^{-1} can be generated much faster and more efficiently than M^{-1}, particularly for problems with a lot of MoM boundary elements.

Since the preconditioning technique requires the FEM/MoM boundary to be located far from the surface of the scatterer, more elements may be required increasing the order of the system of equations. However, in many situations the amount of additional computational resources required by these extra elements is small compared to the resources saved by using this preconditioning technique.

III. SAMPLE PROBLEMS

Four sample problems were used to evaluate the preconditioning techniques discussed in later sections. The first problem is a perfectly conducting (PEC) sphere, which does not require any FEM elements to model. The second problem is a dielectric-coated sphere, where the coating is thin relative to the radius of the sphere. This structure requires both FEM and MOM elements to model. The third problem is a solid dielectric sphere

requiring many more FEM elements. These spherical structures are convenient because they can be modeled analytically. The FEM part of the hybrid system becomes more dominant from the first problem to the third problem. The remaining problem is a printed circuit board (PCB) power bus structure, which is a structure of particular interest to EMC and signal integrity engineers. Each sample configuration is modeled at 3 GHz.

Problem 1: Perfectly Conducting Sphere

The first sample configuration is a perfectly conducting sphere. The radius of the sphere is 8 cm, as shown in Fig. 1. The incident wave travels along the z-axis, and the polarization of the E field is along x-axis. The goal is to model the scattered far fields. The most convenient way to model this structure is to use MoM on the surface of the sphere, so FEM is not required.
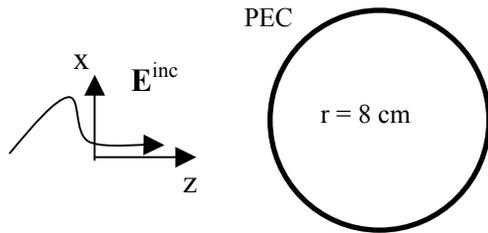
Figure1. Scattering from a PEC sphere.

Problem 2: Dielectric-Coated PEC Sphere

The second configuration is a dielectric-coated PEC sphere. The radius of this sphere is also 8 cm. The coated dielectric material has a thickness of 5 mm (0.05λ at 3 GHz) and relative dielectric constant of $4.0-j1.0$, as shown in Fig. 2. The same incident wave as Problem 1 is applied. The field in the interior of the dielectric material is analyzed using FEM, and the equivalent current on the truncation surface is modeled using MoM.
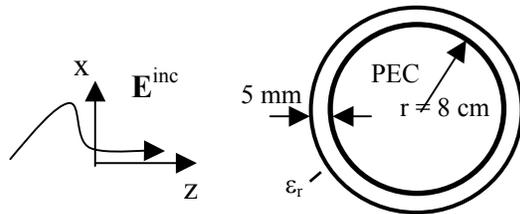
Figure 2. Scattering from a dielectric-coated PEC sphere.

Problem 3: Dielectric Sphere

The third sample configuration is a dielectric sphere. The radius of this sphere is again 8 cm and the relative dielectric constant of the sphere

material is 4.0, as indicated in Fig. 3. The same incident wave as Problem 1 is applied. The field in the interior of the dielectric sphere is analyzed using FEM, and the equivalent current on the truncation surface is modeled using MoM.
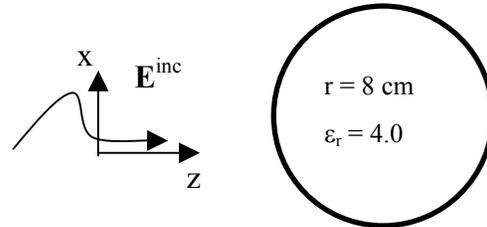
Figure 3. Scattering from a dielectric sphere.

Problem 4: Power Bus Structure

The fourth problem is to model the input impedance of a PCB power bus structure. As shown in Fig. 4, the board dimensions are 30 mm × 20 mm × 2 mm. The top and bottom planes are PECs. The relative dielectric constant of the material between the planes is 4.2. An ideal current source is located at ($x_i = 10$ mm, $y_i = 5$ mm) to excite the structure. Such a structure usually requires a large number of FEM elements between the planes in order to control the aspect ratio of the tetrahedra. This results in a lot of triangular MoM boundary elements if the FEM/MoM boundary is located on the surface of the metal planes.
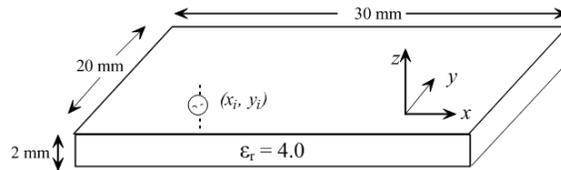
Figure 4. A PCB power bus structure.

Discretization of Sample Structures

Since the MoM provides an exact RBC on the truncation surface, it doesn't matter how far the truncation surface is from the scatterer. However, it is usually convenient to choose the truncation surface to coincide with the physical boundary of the scatterer to minimize the computational domain. Defining the distance between the truncation surface and physical boundary of the scatterer as *d*, Table 1(a) summarizes the discretization of the sample problems when $d = 0$ (i.e., the truncation surface coincides with the physical boundary of the spheres or PCB). The mesh density on this truncation surface is about 10 elements/wavelength. The total number of unknowns is given by the sum of the number of E_i, E_s, and J_s elements.

Table 1. Summary of discretization of the sample problems

(a) when $d = 0$

	# of tetrahedra	# of E_i	# of E_s	# of J_s	Total # of unknowns
Problem 1	0	0	0	2589	2589
Problem 2	5491	3660	2910	2910	9480
Problem 3	6541	6379	2589	2589	11557
Problem 4	456	274	68	552	832

(b) when $d = 5$ mm

	# of tetrahedra	# of E_i	# of E_s	# of J_s	Total # of unknowns
Problem 1	5491	3660	2910	2910	9480
Problem 2	11923	10851	3549	3549	17949
Problem 3	12032	12628	2910	2910	18448
Problem 4	3353	2724	1464	1464	5652

In order for the FEM-ABC preconditioner to be effective, the truncation surface has to be moved away from the physical boundary of the scatterer. In this study, a truncation surface with $d = \lambda/20 = 5$ mm in each direction was used when the FEM/ABC preconditioner was employed. This choice of d should be sufficient to provide a good preconditioner [19]. Table 1(b) summarizes the discretization when $d = 5$ mm. The mesh density on this truncation surface is also about 10 elements/wavelength.

As we can see from Table 1, applying the FEM-ABC preconditioner increases the total number of unknowns roughly by a factor of 2 to 7 for the structures studied in this paper. For the PEC sphere, no FEM elements are necessary when $d = 0$. Only the coefficient matrix C needs to be saved and only MoM is applied in this case. When the truncation boundary is moved away from the surface of the sphere, tetrahedral finite elements are added and the memory requirement at least doubles since the matrix D (which is as dense as the C matrix) also needs to be saved.

For the dielectric-coated sphere, the number of tetrahedral elements roughly doubles when d is increased from 0 to 5 mm. The number of E_i elements roughly triples, and the number of E_s and J_s elements also increases due to the larger surface area.

For the dielectric sphere, there are a large number of tetrahedral elements even when the truncation boundary coincides with the physical

boundary of the sphere. However, the number of unknowns still increases significantly when the truncation surface is extended beyond the physical boundary of the sphere.

For the power bus structure, the thickness of the board requires a fine tetrahedral mesh in the dielectric in order to ensure that the tetrahedra have a reasonable aspect ratio. When d is increased from 0 to 5 mm, many more tetrahedral elements must be used to discretize the computational domain between the physical boundary of the board and the truncation boundary, resulting in a large increase in the total number of unknowns. At lower frequencies (longer wavelengths), the boundary would need to be located even further from the scattering surfaces.

IV. PRECONDITIONING TECHNIQUES

The inverse of the matrix Q in Equation (14) can be used as a preconditioner for iterative solutions of Equation (4). However, it is usually very expensive to derive an explicit inverse of this matrix. An incomplete LU factorization of the matrix Q will result in $Q \approx LU$, where L is a sparse, lower-triangular matrix, and U is a sparse, upper-triangular matrix. The preconditioner, P, is then given by $P = Q^{-1} \approx (LU)^{-1}$, where the inversion is actually replaced by forward and back substitution at each iteration.

There are two popular ILU schemes, one based on the structure of the matrix being factored, and the other based on the numerical values of the

elements in L or U generated during factorization [21]. In the first scheme, an element in L or U is dropped if the element in the corresponding position of the original matrix is zero, no matter how large this element is. In the second scheme, an element in L or U is discarded only if its magnitude is smaller than a specified *drop tolerance*. The second scheme often yields more accurate factorizations than the first scheme. Variations of each scheme and hybridizations of these schemes are also described in the literature [21].

In this study, the LU factorization based on drop tolerance in MATLAB was used [25]. The drop tolerance was set to 1.0×10^{-6} for the results presented here. A smaller drop tolerance yields a more accurate factorization, but produces more fill-in elements. Fill-in elements refer to matrix entries that are zero in the original matrix Q and are nonzero in the L and U matrices. In order to reduce the number of fill-in elements (and the memory required to store these elements), the matrix Q was reordered before the factorization.

Reducing the Number of Fill-ins During ILU by Reordering

There are various reordering algorithms, including variable band, nested dissection and minimum degree [22, 23]. A good variable band algorithm is the reverse Cuthill-McKee algorithm to minimize the bandwidth of a matrix [24]. The minimum degree algorithm is based on graph theory and reduces fill-in elements during Gaussian elimination [25, 26]. In [9], it is shown that the symmetric reverse Cuthill-McKee algorithm (SYMRCM) and symmetric minimum degree algorithm (SYMMMD) effectively reduce the fill-ins during a complete LU on a sparse matrix generated using FEM. In this work, besides the SYMRCM and SYMMMD algorithms, another minimum degree algorithm, the symmetric approximate minimum degree reordering technique (SYMAMD) was also investigated [25]. This algorithm is usually faster than the symmetric minimum degree algorithm and yields a better ordering.

The sparsity pattern of the matrix Q generated using FEM and ABC for Problem 1 (d = 5 mm) is shown in Fig. 4(a). The average number of nonzero elements is about 12 elements per row in this case, which indicates that Q is highly sparse. The sparsity pattern using various reordering algorithms is also shown in Fig. 5.

Table 2 lists the number of nonzero elements in the L and U matrices after an ILU factorization of matrix Q using a drop tolerance of 1.0×10^{-6}. Problems 2 and 3 could not be factored within the available memory without reordering. For L and U using sparse complex values with double precision, the required memory (in bytes) is roughly given by the number of nonzero elements times 20. The memory required to store the L and U matrices is also listed in Table 2. As we can see, the number of fill-in elements during ILU is greatly reduced by reordering the matrix. It is also much faster to perform ILU factorizations when the reordering schemes are applied. On average, the SYMRCM algorithm performed a little better than the other algorithms. This is probably due to the asymmetric nature of the matrix Q.

Iterative Solver Behavior

After L and U are generated, they can be applied to the iterative solver at each iteration and do not have to be explicitly inverted. In this study, a bi-conjugate gradient stabilized (BICGSTAB) solver was utilized [21, 27]. Table 3 summarizes the number of iterations required to achieve a solution with a convergence factor of 1.0×10^{-3}. The convergence factor is the maximum value for the normalized residual norm, $\|Mx - b\|/\|b\|$. In other words, the BICGSTAB solver has converged once $\|Mx - b\|/\|b\| \le 1.0 \times 10^{-3}$ is achieved. The maximum number of iterations investigated in this study was 500.

The general behavior of the BICGSTAB solver is described as being divergent, convergent, or stagnant in Table 3. For divergent behavior, the normalized residual norm bounces between certain values above the required tolerance as the number of iterations increases. For convergent behavior, the normalized residual goes below the tolerance in less than 500 iterations. For stagnant behavior, the normalized residual norm remains the same for two consecutive iterations. The BICGSTAB solver stops the solution process before reaching the maximum number of iterations if stagnant behavior occurs.
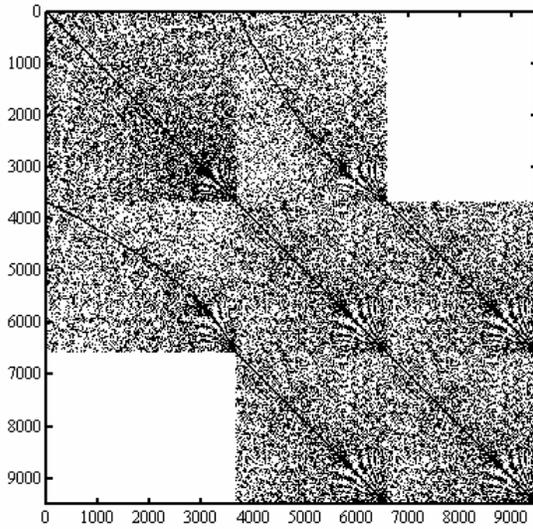
(a) Sparsity pattern of the original matrix Q.
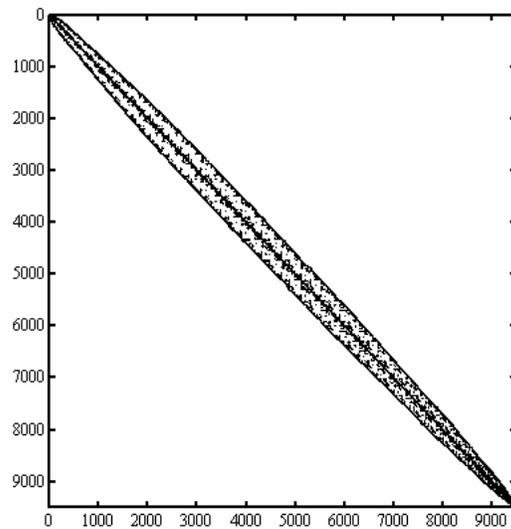
(b) Sparsity pattern of the matrix Q after SYMRCM ordering.
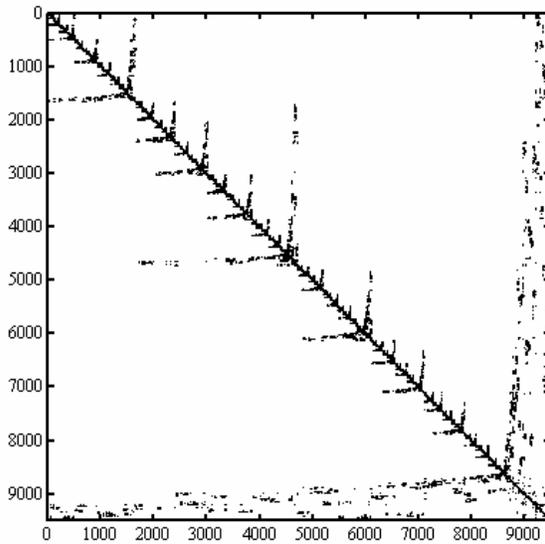
(c) Sparsity pattern of the matrix Q after SYMMMD ordering.
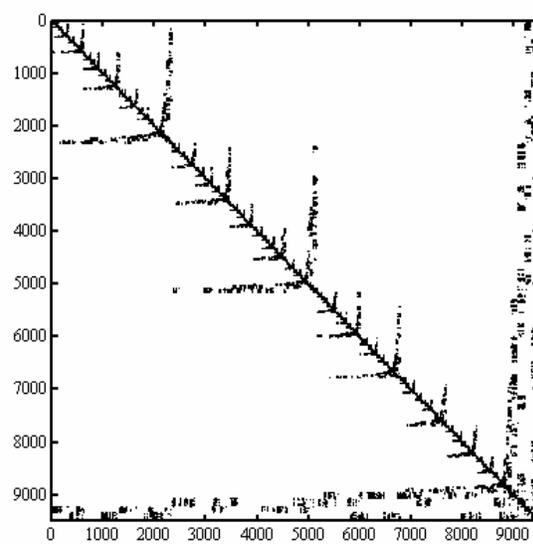
(d) Sparsity pattern of the matrix after SYMAMD ordering.

Figure 5. Sparsity pattern for Problem 1 matrix generated using FEM and ABC.

Table 2. The number of nonzero elements in L and U after ILU

	No ordering (Mbytes)	SYMRCM (Mbytes)	SYMMMD (Mbytes)	SYMAMD (Mbytes)
Problem 1	21151493 (423)	2507653 (50)	2701435 (54)	2710165 (54)
Problem 2	Out of memory	9534816 (190)	10000965 (200)	10415806 (208)
Problem 3	Out of memory	27943414 (559)	33754661 (675)	Out of memory
Problem 4	8875433 (176)	2319723 (46)	2504835 (50)	2437372 (49)

Table 3. Iterations required using un-preconditioned and preconditioned BICGSTAB

	Un-preconditioned BICGSTAB			Preconditioned BICGSTAB		
	# of Iterations	Converged (Yes/No)	General behavior	# of Iterations	Converged (Yes/No)	General behavior
Problem 1	500	No	Divergent	14	Yes	Convergent
Problem 2	500	No	Divergent	14	Yes	Convergent
Problem 3	500	No	Divergent	35	Yes	Convergent
Problem 4	47	No	Stagnant	27	Yes	Convergent

Table 4. Number of nonzero elements in L and U and iterations required to converge when the coupling between FEM and ABC was discarded, and SYMMMD was used

	Problem 1	Problem 2	Problem 3	Problem 4	
				Radiation	Scattering
# of nonzero element in L and U (MBytes)	377965 (8)	2515255 (50)	17715266 (354)	597535 (12)	
# of iterations for convergence	24	26	500 (Did not converge)	103	40
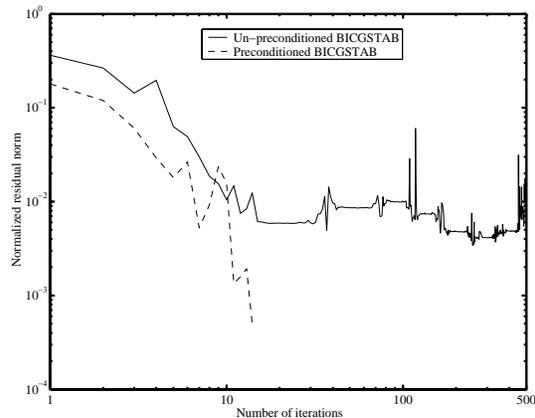
Figure 6. Convergence/divergence curve for Problem 1.

Figure 6 plots the normalized residual norm as a function of the number of iterations for Problem 1 using the un-preconditioned and preconditioned BICGSTAB solver. As we can see, the FEM-ABC preconditioner greatly reduces the number of iterations required for convergence.

Reducing the Number of Fill-ins by Decoupling FEM and ABC

In this study, a modified FEM/ABC preconditioner requiring less memory was also evaluated. In Equation (13), the coupling between FEM and ABC is achieved through the B_{ss} and $B_{ss}{}^{T}$ coefficient matrices. Although the elements in these matrices are bigger than those on the same row in the diagonal entries of the matrix Q, we discarded the B_{ss} and $B_{ss}{}^{T}$ matrices and used the resulting sparse matrix, Q', to construct preconditioners. For scattering problems like Problems 1, 2 and 3, discarding the coupling between the FEM and ABC is effectively the same as imposing a PEC boundary condition on the truncation surface. For radiation problems like Problem 4, discarding the coupling between the FEM and ABC effectively imposes a perfectly magnetically conducting (PMC) boundary condition on the truncation surface.

Discarding the elements corresponding to the coupling between FEM and ABC dramatically reduces the number of fill-ins during ILU factorization. Table 4 lists the number of nonzero elements and the number of iterations required for convergence. The memory required to store the L and U matrices is given in parentheses.

Comparing the results in Table 4 to the results in Tables 2 and 3, we observe that this preconditioner works reasonably well for PEC and dielectric-coated PEC spheres. The number of iterations required to converge is higher, but the memory required is significantly reduced. Since the ABC truncation surface is close to the PEC sphere in both cases, discarding the coupling between the

FEM and ABC (implicitly applying a PEC boundary condition) is a reasonable approximation of the FEM and ABC. Figures 7 and 8 show the calculated radar cross section (RCS) for the PEC sphere in Problem 1 and the dielectric-coated sphere in Problem 2 using the decoupled FEM-ABC as preconditioner, respectively. Analytical results for the RCS of this geometry obtained using the Mie series [29] are also provided. The results obtained using the two methods agree with each other very well.
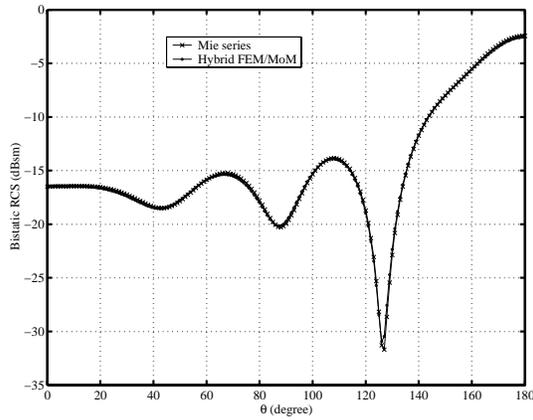
Figure 7. Calculated RCS for Problem 1.
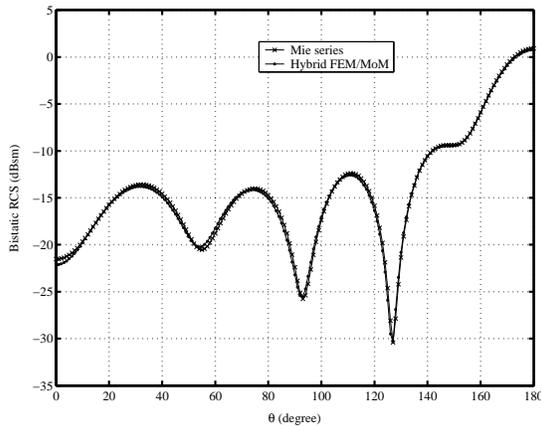
Figure 8. Calculated RCS for Problem 2.

For the PCB power bus structure, the memory was reduced by a factor of 4, however, the number of iterations increased by a factor of 4, as shown in the first sub-column in Table 4 for Problem 4. In this case, the excitation is located inside the FEM region. The preconditioner implicitly applies a PMC boundary condition. To demonstrate the different behavior of the proposed preconditioner

for scattering problems vs. radiation problems, the same configuration was modeled with the incident wave from Problem 1 instead of the internal current source. This change only affects the terms on the right hand side of Equation (4). The memory required by the preconditioners in the scattering case is the same as that in the radiation case. Using the original preconditioner with FEM and ABC coupled together, 17 iterations are required to reach a 1.0×10^{-3} convergence factor. Applying the new preconditioner with FEM and ABC decoupled (i.e. implicitly applying a PEC boundary condition), the memory is still reduced by a factor of 4 and 40 iterations are required to converge.

For the dielectric sphere, the iterative solver did not converge for Problem 3. The normalized residual norm oscillated around 3.0×10^{-3}. Therefore, in this case, discarding the coupling between the FEM and ABC elements resulted in a poorer preconditioner.

Eliminating the coupling terms between the FEM and ABC portions of the preconditioning matrix appears to work pretty well for scattering problems from structures with large metallic surfaces. However, it does not work as well for radiation problems or for modeling structures without large metal surfaces.

V. CONCLUSIONS

In this paper, four sample problems were used to investigate the application of preconditioning techniques to the iterative solution of matrix equations resulting from the hybrid FEM/MoM method employing a combined formulation. These techniques were based on the FEM/ABC, which yields a physical approximation of the geometry being evaluated. An ILU factorization employing a drop tolerance was used to construct the preconditioner. Reordering algorithms reduced the number of nonzero elements in the *L* and *U* matrices by a factor of 4 to 8, depending on the geometry and reordering scheme applied.

When FEM/ABC preconditioners were applied to the solution of the hybrid FEM/MoM system of equations, the convergence rate of the iterative solution improved significantly. These preconditioners work very well for calculating the scattering from PEC spheres (with few FEM elements), dielectric coated spheres, and dielectric spheres (with many FEM elements). They also worked well for modeling radiation and scattering from a PCB power bus structure (with many FEM elements).

The memory required by the preconditioner can limit the size of the problems that can be modeled. This memory requirement can be reduced significantly by discarding the coupling between the FEM and ABC elements in the preconditioner matrix. In our examples, memory was reduced by a factor of 2 to 7. This modified FEM/ABC preconditioning technique worked very well for analyzing the scattering from PEC and dielectric-coated metal spheres. It also worked well for analyzing the scattering from a PCB. However, it did not work well for modeling the radiation from the PCB or for modeling a dielectric sphere. Since this approach implicitly simulates a PEC boundary for scattering problems (or a PMC boundary for radiation problems), it is generally expected to work well for the analysis of scattering from geometries that have a PEC surface near the FEM/MoM boundary.

ACKNOWLEDGEMENT

REFERENCES

[1]   Y. Ji and T. H. Hubing, "On the modeling of a gapped power-bus structure using a hybrid FEM/MoM approach", *IEEE Trans. Electromag. Compat.,* vol. 44, no. 4, pp. 566–569, Nov. 2002.

[2]   X. Yuan, "Three dimensional electromagnetic scattering from inhomogeneous objects by the hybrid moment and finite element method," *IEEE Trans. Microwave Theory Tech.*, vol. 38, pp. 1053–1058, Aug. 1990.

[3]   J.-M. Jin and J. L. Volakis, "Electromagnetic scattering by and transmission through a three-dimensional slot in a thick conducting plane," *IEEE Trans. Antennas Propagat.*, vol. 39, pp. 543–550, Apr. 1991.

[4]   J.-M. Jin and J. L. Volakis, "A hybrid finite element method for scattering and radiation by microstrip patch antennas and arrays residing in a cavity," *IEEE Trans. Antennas Propagat.*, vol. 29, pp. 1598–1604, Nov. 1991.

[5]   M. W. Ali, T. H. Hubing, and J. L. Drewniak, "A hybrid FEM/MOM technique for electromagnetic scattering and radiation from dielectric objects with attached wires," *IEEE Trans. Electromag. Compat.*, vol. 39, pp. 304–314, Nov. 1997.

[6]   J. Angélini, C. Soize, and P. Soudais, "Hybrid numerical method for harmonic 3D Maxwell equations: Scattering by a mixed conducting and inhomogeneous anisotropic dielectric medium," *IEEE Trans. Antennas Propagat.*, vol. 41, pp. 66–76, Jan. 1993.

[7]   L. W. Pearson, A. F. Peterson, L. J. Bahrmasel, and R. A. Whitaker, "Inward-looking and outward-looking formulations for scattering from penetrable objects," *IEEE Trans. Antennas Propagat.*, vol. 40, pp. 714–720, Jun. 1992.

[8]   A. F. Peterson, S. L. Ray, and R. Mittra, *Computational Methods for Electromagnetics*, New York: IEEE Press and Oxford University Press, 1997.

[9]   Y. Ji, H. Wang and T. H. Hubing, "A novel preconditioning technique and comparison of three formulations for the hybrid FEM/MoM method", *Appl. Computat. Electromagn. Soc. (ACES) J.*, vol. 15, pp. 103–114, Jul. 2000.

[10] J.-M. Jin and J. L. Volakis, "A finite element-boundary integral formulation for scattering by three-dimensional cavity-backed apertures," *IEEE Trans. Antennas Propagat.*, vol. 39, pp. 97–104, Jan. 1991.

[11] O. M. Ramahi and R. Mittra, "Finite element solution for a class of unbounded geometries," *IEEE Trans. Antennas Propagat.*, vol. 39, pp. 244–250, Feb. 1991.

[12] J.-M. Jin and V. V. Liepa, "A note on hybrid finite element method for solving scattering problems," *IEEE Trans. Antennas Propagat.*, vol. 36, pp. 1486–1490, Oct. 1988.

[13] X. Yuan, D. R. Lynch, and J .W. Strohbehn, "Coupling of finite element and moment methods for electromagnetic scattering from inhomogeneous objects," *IEEE Trans. Antennas Propagat.*, vol. 38, pp. 386–393, Mar. 1990.

[14] X. Q. Sheng and E. K. Yung, "Implementation and experiments of a hybrid algorithm of the MLFMA–Enhanced FE-BI method for open-region inhomogeneous electromagnetic problems", *IEEE Trans. Antennas. Propagat.*, vol. 50, no. 2, pp. 163–167, Feb. 2002.

[15] R. Coifman, V. Roklin, and S. Wandzura, "The fast multipole method for the wave equation: a pedestrian prescription," *IEEE Antennas Propag. Mag.*, vol. 35, pp. 7–12, June 1993.

[16] J. M. Song and W. C. Chew, "MLFMA for electromagnetic scattering from large complex objects," *IEEE Trans. Antennas Propag.*, vol. 45, pp. 1488–1493, Oct. 1997.

[17] E. Bleszynski, M. Bleszynski, and T. Jaroszewicz, "A fast integral-equation solver for electromagnetic scattering problems", *IEEE AP-S Int. Symp. Dig.*, Seattle, WA, pp. 416–419, June 1994.

[18] X.-Q. Sheng, J.-M. Jin, J. Song, C.-C. Lu, and W.C. Chew, "On the formulation of hybrid finite-element and boundary-integral methods for 3-D scattering," *IEEE Trans. Antennas Propagat.*, vol. 46, pp. 303–311, Mar. 1998.

[19] J. Liu and J.-M. Jin, "A highly effective preconditioner for solving the finite element-boundary integral matrix equation of 3-D scattering", *IEEE Trans. Antennas Propagat.*, vol. 50, no. 9, pp. 1212–1221, Sep. 2002.

[20] Y. Ji, H. Wang, and T. H. Hubing, "A numerical investigation of interior resonances in the hybrid FEM/MoM method", IEEE *Trans. Antennas Propagat.*, vol. 51, no. 2, pp. 347–349, Feb. 2003.

[21] Y. Saad, *Iterative methods for Sparse Linear Systems*, Boston: PWS Publishing Company, 1996.

[22] I. S. Duff, A. M. Erisman and J. K. Reid, *Direct Methods for Sparse Matrices*, Claerndon Press, Oxford, 1986.

[23] J. L. Volakis, A. Chatterjee, and L. C. Kempel*, Finite Element Method for Electromagnetics*, New York: IEEE Press and Oxford University Press, 1998.

[24] E. Cuthill and J. McKee, "Reducing the bandwidth of sparse symmetric matrices," *Proceedings of the 24th National Conference of the ACM*, New Jersey: Brandon Systems Press, 1969.

[25] MATLAB manuals, MATLAB is a product of Mathworks, Inc, U.S.A.

[26] A. George and J. W. H. Liu, *Computer Solution of Large Sparse Positive Definite Systems*, New Jersey: Prentice-Hall, 1981.

[27] R. Barrett, M. Berry, T. F. Chan, F. Demmel, J. M. Donato, J. Dongarra, V. Eijkhout, R. Pozo, C. Romine, and H. Van der Vorst, *Templates for the Solution of Linear Systems: Building Blocks for Iterative Methods*, Philadelphia: SIAM, 1994.

[28] C. Guo and T. H. Hubing, "Development and application of a fast multipole method in a hybrid FEM/MoM field solver", *Journal of the Applied Computational Electromagnetics Society*, vol. 19, no. 3, pp. 126-134, Nov. 2004.

[29] W. C. Chew, *Waves and Fields in Inhomogeous Media*, New York: IEEE Press, 1995.

Chunlie Guo earned his BSEE and MSEE degrees from Tsinghua University in 1998 and 2000, respectively. He is currently pursuing a Ph.D. degree in Electrical Engineering at the University of Missouri-Rolla. His graduate research is focused on the development of numerical modeling techniques for analyzing signal integrity and electromagnetic compatibility problems.

Todd Hubing received his BSEE degree from MIT in 1980, his MSEE degree from Purdue University in 1982, and his Ph.D. in Electrical Engineering from North Carolina State University in 1988.

From 1982 to 1989, he was an electromagnetic compatibility engineer for IBM in Research Triangle Park, NC. He is currently a Professor of Electrical and Computer Engineering at the University of Missouri-Rolla. He serves on the Board of Directors and is a Past President of the IEEE EMC Society.